Study of the 6-Pronged π^+p Interactions at 5 GeV/c

H. Drevermann, U. Idschok, G. Winter, and K. Böckmann
Physikalishes Institut der Universität Bonn, and Kernforschungsanlage Jülick, Bonn, Germany

AND

A. J. Apostolakis, G. Briggs, C. A. Kitchen, and J. V. Major
Department of Physics, University of Durham, Durham, England

AND

C. L. Pols, J. Schotanus, D. Toet, and R. T. Van de Walle
Fysich Laboratorium, R. K. Universiteit Nijmegen, Nijmegen, Holland

AND

R. Lestienne and P. Fleury
Ecole Polytechnique, Paris, France

AND

C. Grosso, B. Quassiati, G. Rinaudo, and A. Werbrouck
Istituto di Fisica dell' Universita, Torino, Italy
and
Istituto Nazionale di Fisica Nucleare, Sezione di Torino, Torino, Italy

(Received 24 March 1967)

As a contribution to the study of high-multiplicity phenomena, we have analyzed 3502 six-charged-prong π^+p interactions observed in a hydrogen bubble chamber; the incident π^+ momentum was 5 GeV/c. The total cross section for this multiplicity is $\sigma = 1.33\pm0.05$ mb, mostly contributed by the following reactions: (A) $\pi^+p \to p3\pi^+2\pi^-$ (0.40 ± 0.03 mb), (B) $\pi^+p \to p3\pi^+2\pi^-\pi^0$ (0.61 ± 0.04 mb), and (C) $\pi^+p \to n4\pi^+2\pi^-$ (0.11 ± 0.02 mb). Individual particle momentum distributions, when compared with Lorentz-invariant statistical phase space, display deviations which are rather weak but still quite significant. The ρ^0 meson is abundantly produced in the first reaction (0.26 ± 0.05 mb). In the second reaction the ω meson is seen with a comparable cross section (0.26 ± 0.03 mb); χ^0 and η are also observed (50 ± 20 μb and 100 ± 20 μb, respectively, after correction for neutral decays). For both ρ^0 and ω resonances there is indication of spin alignment. $N^{*++}(1236)$ production is quite strong; the rate estimate is made difficult by the presence of distortions of the mass spectrum that are shown to be mostly concerned with the π^+p combinations of low c.m. velocity. It is suggested that the short lifetime of the $N^*(1236)$ resonance has some bearing on this effect, which indeed seems to affect also the ρ^0 and not the longer-lived ω.

I. INTRODUCTION

In πp interactions the interest is focused mostly on low-multiplicity phenomena (two or four charged secondary tracks). Recently investigations on high-multiplicity interactions have been made between 4 and 10 GeV/c.[1–5] Here we report on reactions with six charged secondary tracks in collisions of 5 GeV/c π^+ with protons. Preliminary results have already been presented.[6]

In this paper we describe, firstly, some experimental details and the procedures which lead to the classification of the events into channels according to the kinematical fits and the determination of the corresponding partial cross sections. Secondly, the distributions of individual final-state particles are considered and compared with the predictions of relativistic statistical phase space. This is followed by an examination of resonance production in the two most populated channels, namely channel A ($\pi^+p \to p+5\pi$) and channel B ($\pi^+p \to p+6\pi$). The angular decay distributions of the three abundantly produced resonances N^*, ρ^0, and ω are studied next. (Hereafter N^* means $N_{3/2,3/2}{}^{*++}(1236)$ unless otherwise specified.) In particular, evidence is sought for possible spin alignments. A significant distortion of the N^* peak was found to be related to the center-of-mass (c.m.) velocity of the N^*; a similar examination was effected for the ρ^0 and ω mesons and some speculations are presented on the physical meaning of this velocity dependence. Finally there is a brief description of the less populated channels.

[1] J. Bartke, A. Eskreys, G. Pytkowicz, K. Zalewski, M. Bardadin, L. Michejda, S. Otwinowski, and R. Sosnowski, Institute of Nuclear Research (Warsaw) Report No. INR 597 VI/PH, 1965 (unpublished).

[2] M. Bardadin-Otwinowska, L. Michejda, S. Otwinowski, and R. Sosnowski, Phys. Letters **21**, 351 (1966).

[3] P. Slattery and H. Kraybill, Bull. Am. Phys. Soc. **11**, 55 (1966); (private communication).

[4] L. Bondár, K. H. Eickel, H. Kaufmann, K. Lanius, R. Leiste, R. Pose, K. Böckmann, U. Gorsch, K. Steinberger, B. Nellen, V. Blobel, H. Butensch, I. Damann, P. V. Handel, E. Lohrmann, P. Schilling, G. Wolf, N. N. Biswas, N. Schitz, and I. Weigl, Desy Report No. 66/11, 1966 (unpublished); Nuovo Cimento **44**, 530 (1966).

[5] M. Bardadin-Otwinowska, M. Danysz, T. Hofmokl, S. Otwinowski, H. Piotrowska, R. Sosnowski, M. Szeptycka, and A. Wroblewski, Institute of Nuclear Research (Warsaw) Report No. INR 761/VI/PH, 1966 (unpublished); (private communication).

[6] Bonn, Durham, Nijmegen, Paris (E.P.), Turin Collaboration, in *Proceedings of the Oxford International Conference on Elementary Particles* (Rutherford High Energy Laboratory, Harwell, England, 1966), Abstract A, p. 72.

II. METHODS AND RESULTS

1. Experimental Procedure and Cross Sections

The experiment has been carried out at the CERN proton synchrotron using an electrostatically separated beam of π^+ mesons whose momentum was 5.0 GeV/c with a spread of $\pm 0.5\%$. During the exposure of the 150-cm British National hydrogen bubble chamber (BNHBC), 125 000 good pictures were taken with an average flux of 12 tracks per picture. For event selection, a fiducial region with a length of 70.4 cm was chosen in order to obtain a minimum track length of 40 cm for forward secondary tracks.

Among the approximately 3800 six-prong events scanned, about 10% could not be analyzed because of measuring difficulties. The scanning loss was estimated to be less than 1%, by scanning each roll twice. Analysis was carried out using the geometrical reconstruction program THRESH and the kinematical fitting program GRIND. Pions and protons were distinguished by ionization up to a momentum of 1.5 GeV/c in favorable cases. A χ^2 cutoff of $\chi^2<24$ was applied to four constraint (4C) fits whereas for the one constraint (1C) fits the limit was $\chi^2=6$. In the case of an ambiguity between a 4C and a 1C fit the 4C fit was always preferred, as suggested by FAKE[7] calculations, provided it was consistent with ionization. In all other remaining ambiguous cases ($\sim 5\%$) the hypothesis with the lowest χ^2 was chosen. Those events without an acceptable fit to any hypothesis were assumed to have more than one neutral secondary particle, and were classified further by ionization when possible.

In Table I, the total number of events for each reaction and the corresponding cross sections are given. The latter were obtained from the number of events and beam tracks inside the fiducial volume using a hydrogen density of 0.0608 and correcting for beam attenuation and 3% muon contamination. For the cross sections of Table I events remaining ambiguous between the channels D and E were counted half in each channel.

Figure 1 displays the variation of the total and partial cross sections for channels A, B, and C as a function of incident pion momentum.

2. Final-State Particles

2.1 Center-of-Mass Distributions and Statistical-Model Predictions

The distributions of the components P_x and P_y of the center-of-mass momenta[8] for the particles in the six-prong reaction

$$\pi^+p \rightarrow p3\pi^+2\pi^- \text{ (channel } A\text{)}$$

are shown in Fig. 2(a). Here P_x is the component of momentum (longitudinal momentum) of a given particle along the direction of the incoming primary in the center-of-mass and P_y is the component along a fixed, but arbitrary axis, orthogonal to it. Relative to the corresponding distributions at lower multiplicity in this experiment (i.e., $\pi^+p \rightarrow p2\pi^+\pi^-$) shown in Fig. 2(b), the distributions for the six-prong events are much closer to the statistical-model predictions. For the other channels B, C, D, and E, a similar conclusion may be drawn.

In contrast to observations at lower multiplicity, there is no strong evidence from the nucleon and pion distributions for peripheralism[9] in the six-prong events; that is, there is no obvious concentration of events in the region of small P_y and large $|P_x|$. However, there

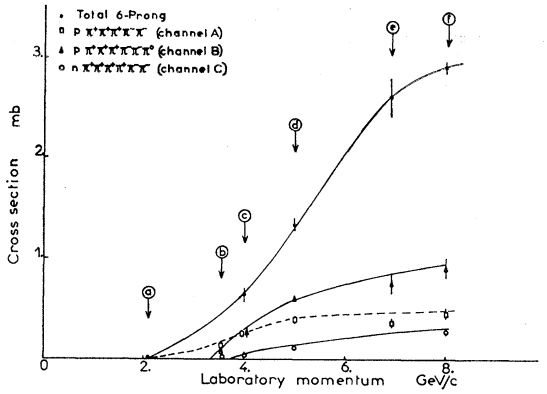

FIG. 1. Variation with energy of the total and partial cross sections (channels A, B, and C) for six-charged-prong events. This figure has already been presented by Bardadin-Otwinowska *et al.* (Ref. 5). (a) F. James and H. Kraybill, Phys. Rev. **142**, 896 (1966); (b) D. D. Carmony, D. N. Hoa, R. L. Lander, C. Rindfleisch, and Wg. H. Young, in *Proceedings of the International Conference on High Energy Physics, Dubna, 1964* (Atomizdat, Moscow, 1965), Abstract No. VII, p. 67; (c) L. Bondàr *et al.* (Ref. 4); (d) this experiment; (e) P. Slattery *et al.* (Ref. 3); (f) Bardadin *et al.* (Ref. 5).

TABLE I. Cross sections for the various six-charged-prong reactions.

Channel	Reaction	No. of events	Cross section (mb)
A	$p\pi^+\pi^+\pi^+\pi^-\pi^-$	1055	0.41±0.02
B	$p\pi^+\pi^+\pi^+\pi^-\pi^-\pi^0$	1597	0.61±0.03
C	$n\pi^+\pi^+\pi^+\pi^+\pi^-\pi^-$	279	0.11±0.01
D	$p\pi^+\pi^+\pi^+\pi^-\pi^-+i\pi^0$, $i>1$	378	0.15±0.01
E	$n\pi^+\pi^+\pi^+\pi^+\pi^-\pi^-+m\pi^0$, $m\geq 1$	140	0.05±0.01
Total		3502	1.33±0.05

[7] G. Lynch, University of California Lawrence Radiation Laboratory Report No. UCRL 10335, 1962 (unpublished).

[8] The P_x, P_y (rather than P_L, P_T) representation is chosen because it displays more readily the symmetry (or asymmetry) of the c.m. distribution of particles since P_x and P_y are equivalent in statistical predictions.

[9] The concept of peripheralism is quite clear in quasi-two-body reactions. It is characterized by a strong forward/backward structure in the c.m. system or by the related low-Δ^2 concentration in $d\sigma/d\Delta^2$ plots and is generally interpreted by meson exchange. For interactions resulting in high multiplicity the above definitions are not synonymous implying that in the present context it is necessary to define "peripheralism" every time that it is used.

TABLE II. Parametrizations of the distributions of single particles observed in this experiment.

Channel	$\langle P_x \rangle$ (MeV)	σ_x (MeV)	σ_y (MeV)	a_x	b_x	b_y	$\langle P_T \rangle$ (MeV)	$\langle P^* \rangle$ (MeV)	$\langle P_{\text{lab}} \rangle$ (GeV)	A_s
					Nucleon					
A	−183±19	403±13	318±10	−0.50±0.05	1.08±0.04	0.87±0.03	396±10	590±16	1.48±0.04	−0.34±0.03
B	−168±13	356±10	298± 8	−0.52±0.04	1.11±0.03	0.93±0.03	372± 8	545±13	1.47±0.04	−0.34±0.02
C	−162±35	343±25	222±20	−0.51±0.11	1.07±0.08	0.91±0.06	353±20	512±32	1.45±0.09	−0.42±0.07
D	−192±25	311±18	245±15	···	···	···	320±18	474±22	1.35±0.06	−0.49±0.04
					Positive pions					
A	34± 7	270± 5	234± 4	0.11±0.03	1.09±0.02	0.94±0.02	286± 4	382± 6	0.79±0.01	0.05±0.02
B	14± 5	214± 3	200± 3	0.07±0.02	1.02±0.01	0.95±0.01	265± 3	318± 4	0.65±0.01	0.06±0.01
C	39±10	224± 7	190± 6	0.19±0.05	1.10±0.04	1.04±0.03	256± 6	335± 9	0.71±0.02	0.07±0.04
D	14± 8	164± 6	161± 5	···	···	···	202± 5	262± 8	0.55±0.02	0.05±0.03
E	23±10	168± 7	171± 8	···	···	···	207± 6	273± 9	0.58±0.02	0.07±0.04
					Negative pions					
A	50± 9	282± 6	234± 5	0.20±0.04	1.13±0.02	0.94±0.02	286± 5	391± 8	0.84±0.02	0.11±0.02
B	39± 6	214± 4	193± 4	0.19±0.03	1.02±0.02	0.92±0.02	237± 4	313± 6	0.69±0.01	0.15±0.02
C	3±12	187± 8	155± 7	0.02±0.06	0.91±0.04	0.88±0.03	219± 7	284±11	0.57±0.02	0.04±0.05
D	2± 9	165± 7	155± 6	···	···	···	192± 6	275±10	0.56±0.02	0.12±0.04
E	10±12	163± 8	153± 8	···	···	···	195± 7	250±12	0.53±0.02	0.14±0.06
					Neutral pions					
B	47± 8	221± 6	193± 5	0.23±0.04	1.05±0.03	0.92±0.02	232± 5	314± 8	0.70±0.02	0.19±0.03

is some asymmetry in the plots of P_x and P_y most apparent for the nucleon, in that whereas the y projections of momenta are very similar to the predictions of the statistical model, the x projections have their center of gravity displaced in the backward direction for the nucleons and in the forward one for the pions.

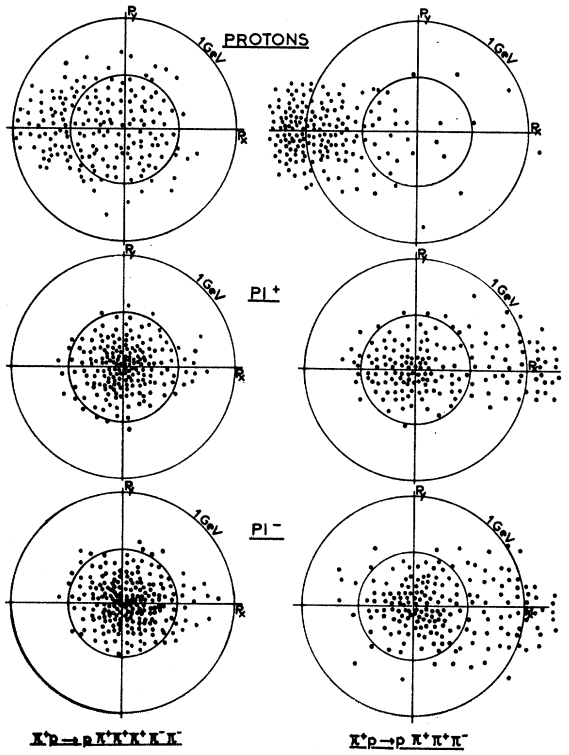

FIG. 2. (a) At left, P_x versus P_y distributions for the outgoing particles in c.m. system for channel A ($\pi^+p \to p\pi^+\pi^+\pi^+\pi^-\pi^-$); (b) at right, the same for the four-body reaction $\pi^+p \to p\pi^+\pi^+\pi^-$. P_x is the projected momentum along the incident direction, P_y is orthogonal to it. Each point represents approximately 1/200 of the available statistics.

The forward displacement for positive pions is significantly smaller than that for negative pions in channels A and B whereas the opposite is the case for channel C (Table II). This could be accounted for by the abundant production in the backward directions of N^{*++} in channels A and B and N^{*-} in channel C. (See Secs. 3, 4, and 7.)

Plotted in Figs. 3(a) and 3(b) are c.m. distributions of P_p^* and $\cos\theta_p^*$ for protons in channels A and B. The angular distributions show considerable backward peaking. As an estimate of the contributions from peripheral collisions to these distributions, it has been proposed to use the asymmetry parameter A_s [where $A_s=(F-B)/(F+B)$], whose values are given in Table II. It should be noted that in the corresponding Δ^2 distribution [Fig. 3(c)] there is a deviation towards the small Δ^2 values, but there is no clear-cut division into a region of peripheral collisions and a region of central collisions. In any case the backward peaking is related firstly, to the over-all shift along P_x and secondly, to the elongation of the distribution in the x direction. At this stage, we prefer to describe the distributions of P_x and P_y in terms of the following parameters:

(a) displacement $a_x=\langle P_x \rangle/\sigma_{\text{stat}}$

and

(b) elongation $b_x=\sigma_{P_x}/\sigma_{\text{stat}}$
$=(\langle P_x^2 \rangle-\langle P_x \rangle^2)^{1/2}/\sigma_{\text{stat}}$,

where σ_{stat} is the rms deviation of the P_x distribution predicted by the statistical model which also predicts $a_x=0$ and $b_x=1$.

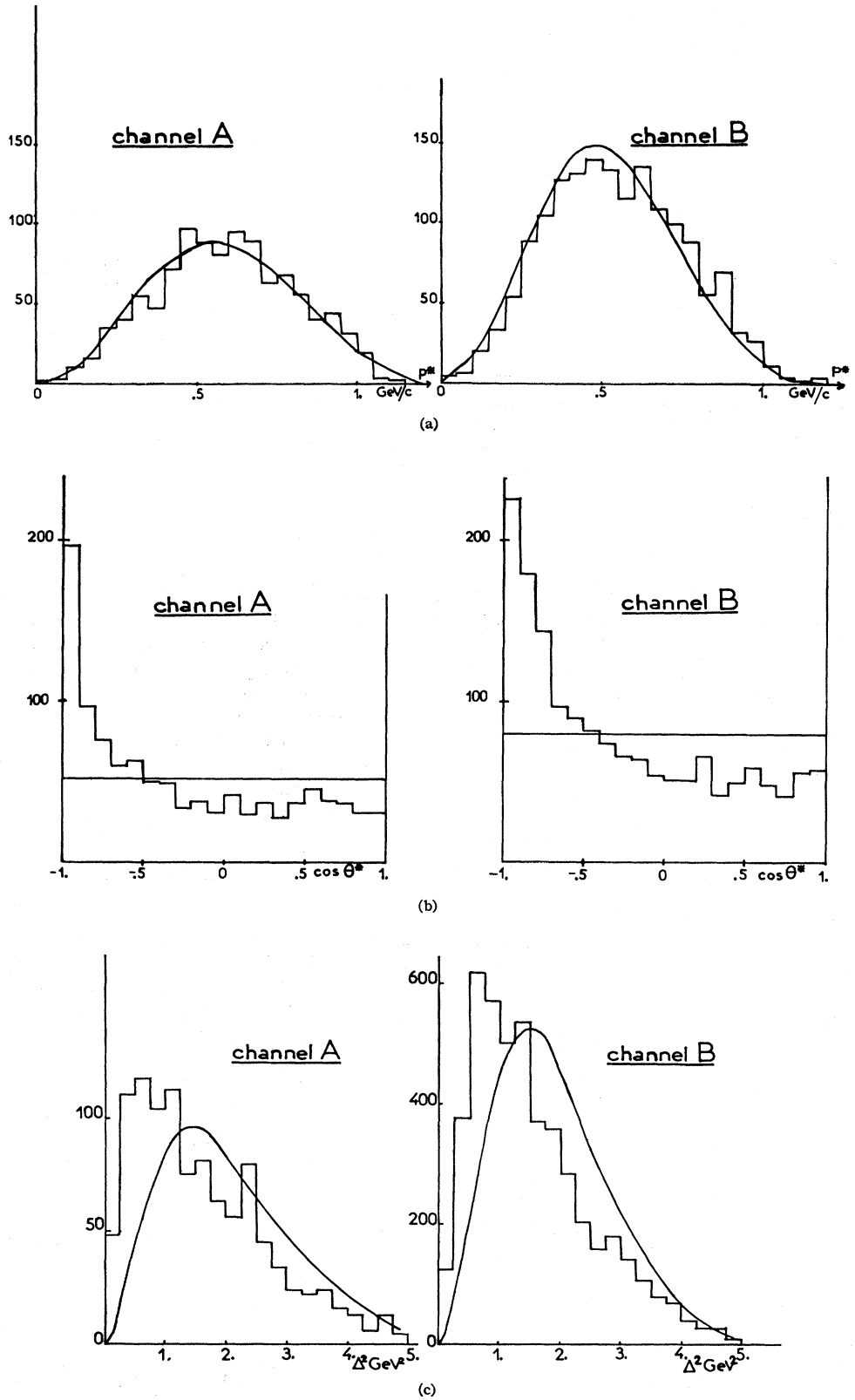

FIG. 3. Center-of-mass distributions of the protons in channels A and B: (a) momentum P^*; (b) scattering angle $\cos\theta^*$; (c) four-momentum transfer Δ^2 from the incident proton. The curves give the predictions of the Lorentz-invariant phase space.

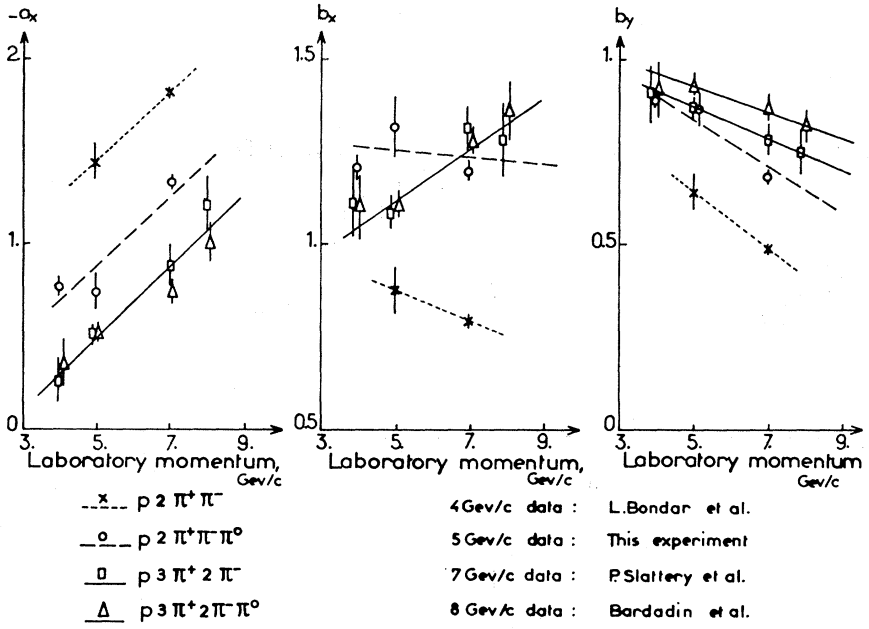

FIG. 4. (a) Variation with energy and multiplicity of the displacement parameter a_x of the nucleon; (b) and (c), variation with energy and multiplicity of the elongation parameters b_x and b_y of the nucleon. (For the definition of these parameters, see Sec. II 3.)

A similar definition of the elongation parameter b_y may be made for the P_y distribution. b_y is much closer to unity than at higher energies for this multiplicity [Fig. 4(c)]. This is probably because the well-known limit ($\sim$300 MeV/c) on the transverse momentum is felt only slightly, since the statistical-model distribution of P_T at 5 GeV/c is comparable to that actually observed at higher energies.

Some authors[2] have investigated the variation of the average values of the transverse momentum $\langle P_T \rangle$ as a function of the longitudinal momentum P_L ($=P_x$) of the outgoing particles. Such plots for the six-prong events are shown in Fig. 5: There is a slight depression of $\langle P_T \rangle$ for low values of P_L for pions and an almost constant value of $\langle P_T \rangle$ for protons. These relationships of $\langle P_T \rangle$ with P_L are expected from the Lorentz-invariant statistical model.

Table II also includes the observed values of the previously defined parameters $\langle P_x \rangle$ or $\langle P_L \rangle$, σ_x, σ_y, a_x, b_x, and b_y for all channels besides the more usual parameters $\langle P_T \rangle$, $\langle P^* \rangle$, $\langle P_{\text{lab}} \rangle$, and A_s. The C channel is restricted to 1C events with $0.76 < \text{MM}^2 < 1.00$ GeV^2 in order to lower contamination.

2.2 Angular Correlations between Particles

It was pointed out originally by Goldhaber *et al.*[10] for $\bar{p}p$ annihilations, and recently by Bartke *et al.*[11] for $\pi^+ p$ interactions at 8 GeV/c, that the distributions of the c.m. angles between pairs of pions depend on whether the pions have like or unlike charges.[12] From the data available in channels A and B, the distributions of the relative angle between pions in the over-all c.m. system are plotted in Fig. 6. In terms of $\gamma = B/F$, one obtains the results given in Table III.

Whereas the γ values tend to differ from γ_{stat} in the sense predicted in Ref. 10, the observed values of γ^{++} and γ^{--} differ from each other, and γ^{+0} and γ^{-0} are less than γ_{stat}. These deviations may be due to the abundant production of resonances in both channels.

2.3 Models of Interaction

The shifts of central values of longitudinal momenta P_x could be accounted for by a model implying two centers of emission (the fire-ball model).[13] Then, in their respective channels A and B, most π^- and π^0 mesons would contribute to the forward center, since they have the larger forward shift; protons would contribute mostly to the backward center and the π^+ mesons to both. This suggestion is supported by very abundant production of the N^* isobar, which is observed predominantly in the backward direction. However, an analysis along these lines meets with some fundamental difficulties. In particular the shifts of the P_x central values are less than the widths of the distributions, that is, the average relative velocity of the centers would be smaller than the velocity of the emitted particles. Consequently the physical meaning of the

[10] G. Goldhaber, S. Goldhaber, W. Lee, and A. Pais, Phys. Rev. **120**, 300 (1960).

[11] J. Bartke, O. Czyzewski, J. A. Danysz, A. Eskreys, J. Loskiewicz, P. Malecki, J. Zaorska, K. Eskreys, K. Juszczak, D. Kisielewska, W. Zielinski, M. Szeptycka, K. Zalewski, G. Pichon, and M. Rumpf, Phys. Letters **24B**, 163 (1967).

[12] Because of Bose-Einstein statistics, like pions tend toward each other, unlike pions tend away from each other more than predicted by statistical phase space.

[13] J. Gierula, Fortsch. Physik **11**, 109 (1963); G. Cocconi, in *Proceedings of 1962 Annual International Conference on High Energy Nuclear Physics at* CERN, edited by J. Prentke (CERN, Geneva, 1962), p. 883.

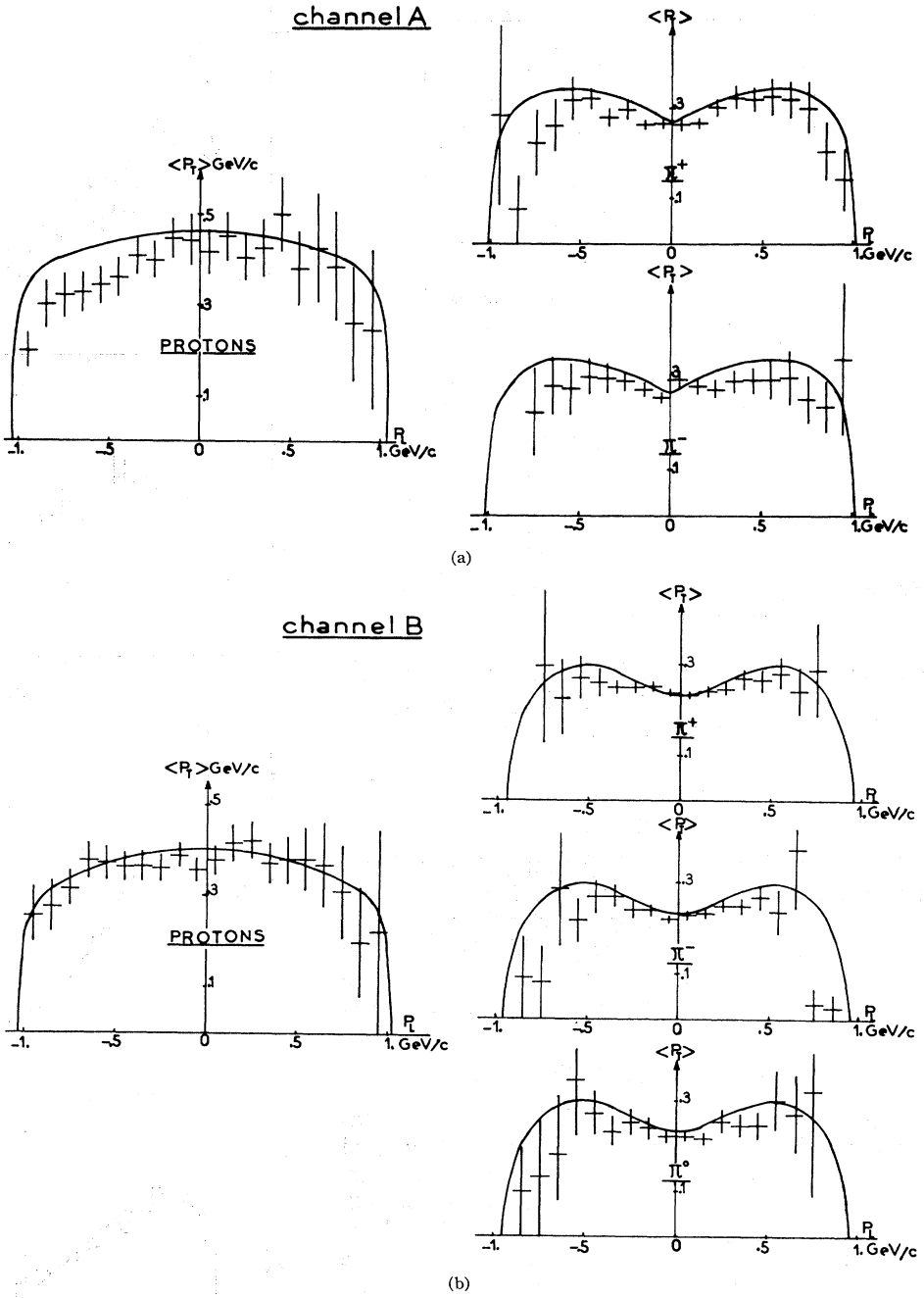

FIG. 5. P_x versus $\langle P_T \rangle$ of the outgoing particles in channels A and B. The curves give Lorentz-invariant phase-space predictions.

two-center model becomes questionable in this context. Another description might be the Landau dynamical model[14] with a single excitation volume. In this model the formation of shock waves is expected in the forward

TABLE III. Angular correlation parameter (B/F ratio) for pairs of pions observed in channels A and B.

Channel	γ^{++}	γ^{--}	γ^{+-}	γ^{+0}	γ^{-0}	$\gamma^{\pi\pi}$ [a]	γ_{stat}
A	1.19±0.04	0.99±0.07	1.71±0.04	···	···	1.45±0.03	1.40±0.02
B	1.23±0.04	1.05±0.06	1.47±0.03	1.26±0.04	1.16±0.05	1.30±0.02	1.31±0.05

[a] Irrespective of charge.

[14] Z. Koba, Progr. Theoret. Phys. (Kyoto) **17**, 288 (1957).

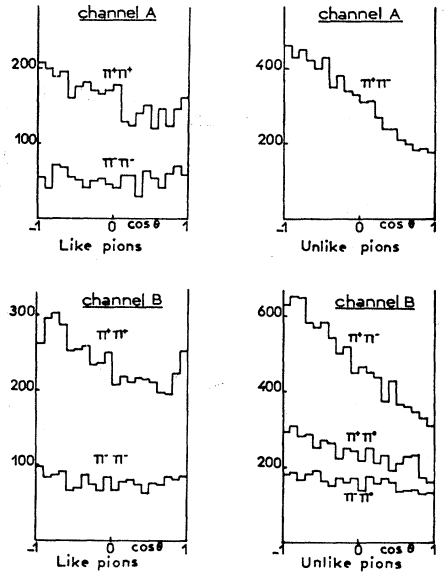

FIG. 6. (a) Distributions of the c.m. angle between pairs of pions in channel A; (b) same for channel B.

and backward directions, but this model does not predict the observed fact that the baryons belong predominantly to the backward shock wave.

3. Resonance Production in the Reaction $\pi^+p \to p3\pi^+2\pi^-$

This channel is dominated by strong N^* and ρ^0 production, which will be discussed in detail below. No other known resonances show up significantly in the effective-mass plots, except for a possible $f^0 \to 4\pi$ signal which will be discussed in conjunction with its observation in the $\pi^+\pi^-$ mode (four-prong events) in a later publication.

3.1 N^* Production

In Figs. 7(a) and 7(b) the effective-mass distributions for the $p\pi^+$ and $p\pi^-$ systems are given. Very good agreement between the observed and phase-space distribution is seen for the case of the $p\pi^-$ system with χ^2 probability of 53%. However in the $p\pi^+$ combinations, there is considerable enhancement above phase-space predictions in the region of the N^* mass. The proportion of N^* production has been estimated by fitting the $p\pi^+$ mass distribution by a sum of two phase-space distributions $d\sigma_1$ and $d\sigma_2$ for the final states $p3\pi^+2\pi^-$ and $N^*2\pi^+2\pi^-$. The N^* distribution was represented by a modified Breit-Wigner function proposed by Jackson[15]:

$$d\sigma_2 \propto \frac{m}{q} \frac{\Gamma(m)}{(m^2-m_0^2)^2+m_0^2\Gamma^2(m)} d\sigma_1.$$

Where m is the effective $p\pi^+$ mass, $m_0=1236$ MeV, q is

[15] J. D. Jackson, Nuovo Cimento **34**, 1644 (1964).

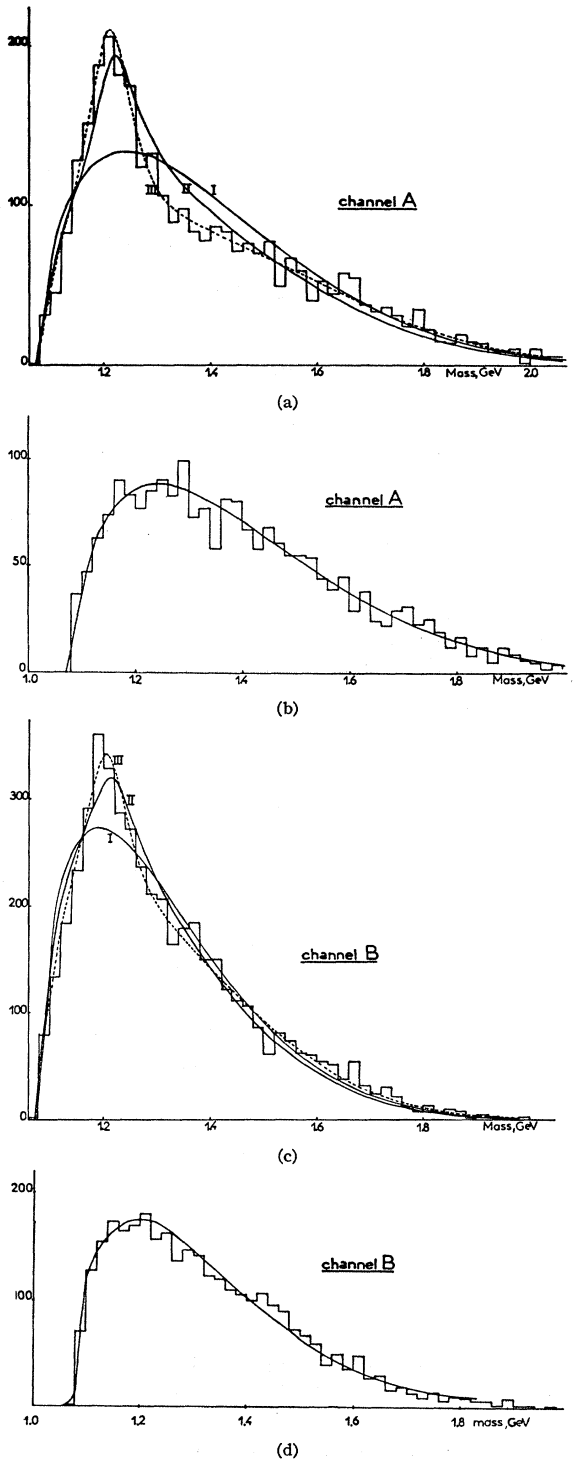

FIG. 7. (a) $p\pi^+$ effective-mass distribution in channel A. Curve I is the purely statistical phase-space prediction; curve II is the best fit obtained, using phase-space and modified Breit-Wigner (Ref. 15) for the $N^*(1236)$; curve III (dashed) gives the best fit obtained when multiplying the latter Breit-Wigner function by a polynomial expansion $[1+\Sigma_{i=1}^{3}a_i(m-m_0)^i]$. (b) $p\pi^-$ effective-mass distributions in channel A. Curve shows the pure phase-space prediction. (c) and (d) are the similar plots and curves for the channel B.

the π momentum in the $p\pi^+$ c.m. system, q_0 is the same at $m=m_0$, and

$$\Gamma(m)=\Gamma(m_0)(q/q_0)^3(am_\pi^2+q^2)/(am_\pi^2+q_0^2),$$

where $\Gamma(m_0)=120$ MeV, m_π is the pion mass, and a was taken as 0.15, i.e., the average of the two Jackson values. The result of the fit leads to a proportion for N^* production of 0.51 ± 0.10.[16]

The χ^2 probability for this fit is very low ($\sim10^{-4}$), and this partly results from the fact that it is not possible to account for the shift of the peak of the N^* mass from 1223, as predicted by the above formula, to about 1210 MeV. A good fit can be obtained by multiplying the Breit-Wigner term by a factor $1+\sum a_i(m-m_0)^i$ with $i\leq3$ and where the a_i parameters are determined in the fitting. This expansion of the Breit-Wigner term is equivalent to allowing for some unknown contribution to the $p\pi^+$ mass plot and results in a χ^2 probability of 67%. Interpreting the zero-order term of the expansion as the N^* isobar leads to a new estimate of the proportion of N^* produced. This is 0.60 ± 0.10, corresponding to a cross section of 0.25 ± 0.05 mb.

3.2 ρ^0 Production

In Figs. 8(a), 8(b), 8(c) the effective-mass distributions of the dipion systems ($\pi^+\pi^-$, $\pi^+\pi^+$, and $\pi^-\pi^-$) are shown. Since six combinations of $\pi^+\pi^-$ enter into the histogram for each event, the ρ^0 meson shows up only as a relatively weak enhancement. The proportion of ρ^0 production was estimated by fitting a sum of the two-phase space distributions for the final states $p3\pi^+2\pi^-$ and $p2\pi^+\pi^-\rho^0$. Again a modified Breit-Wigner distribution for the ρ^0 decay was used.[15] The fit results in a proportion of ρ^0 of (0.63 ± 0.12), corresponding to a cross section of (0.26 ± 0.05) mb. The probability of the χ^2 fit is $\sim10^{-3}$. The low-mass excess in the $\pi^+\pi^+$ and $\pi^-\pi^-$ mass distributions is compatible with the above mentioned angular correlation between like pions (Sec. 2.2).

3.3 Simultaneous Production of N^* and ρ^0

The determination of the fraction of events in which the N^* and ρ^0 are produced simultaneously is made difficult by the many combinations involved and the peaking of phase space in the N^* region.

By fitting the two-dimensional plot of $M(P\pi_1^+)$ versus $M(\pi_{2,3}^+\pi^-)$, the simultaneous production of N^* and ρ^0 is estimated to take place in 0.50 ± 0.11 of the events. This result is consistent either with statistical overlap ($\sim40\%$) or with full correlation ($\sim60\%$).

3.4 C.m. Angular Dependencies of Resonance Production

By observing the angular distributions of the individual particles in the c.m. system, it has been estimated in Sec. 2.1 that the main part of the reactions proceed via central collisions, despite forward and backward peaking. However, it is interesting to examine how this peaking is related to the abundant N^* and ρ^0 production.

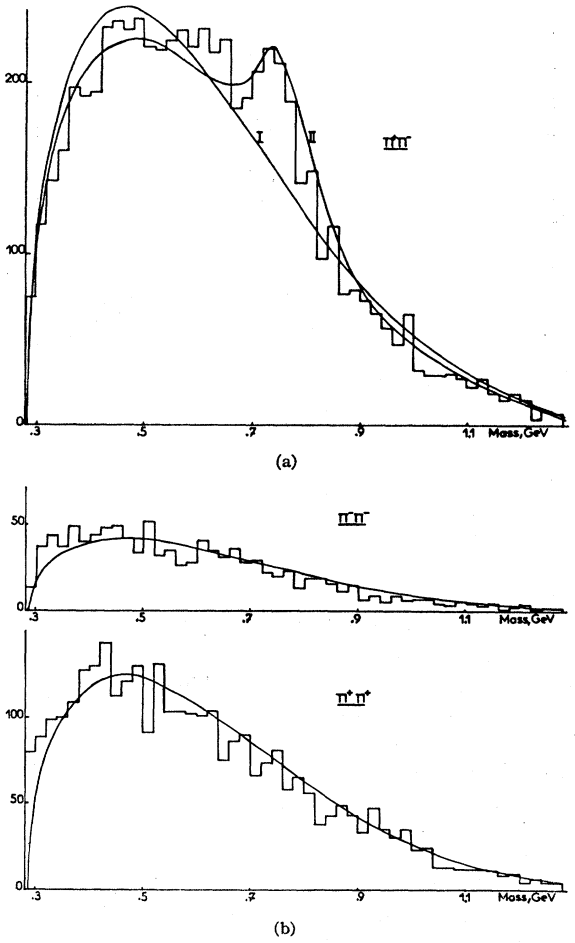

FIG. 8. (a) $\pi^+\pi^-$ effective-mass distribution in channel A. Curve I represents pure phase space and curve II gives the best fit obtained summing the two-phase-space distribution for the final states $p3\pi^+2\pi^-$ and $p2\pi^+\pi^-\rho^0$ [the ρ^0 decay function includes centrifugal barrier (Ref. 15); the ρ^0 reflection is taken into account]. (b) $\pi^-\pi^-$, (c) $\pi^+\pi^+$ effective-mass distributions in channel A. The curves give pure phase-space predictions.

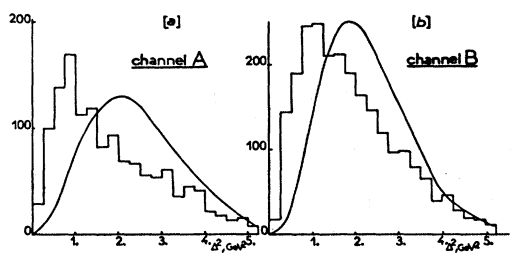

FIG. 9. (a) $\partial N/\partial\Delta^2$ spectrum for π^+p combinations in the N^* band ($1.12<M\pi^+p<1.30$ GeV) in channel A. The curve represents the phase-space predictions. (b) same for channel B.

[16] The errors on quantities determined by minimum χ^2 are estimated from the width of the χ^2 curve in the region of the minimum.

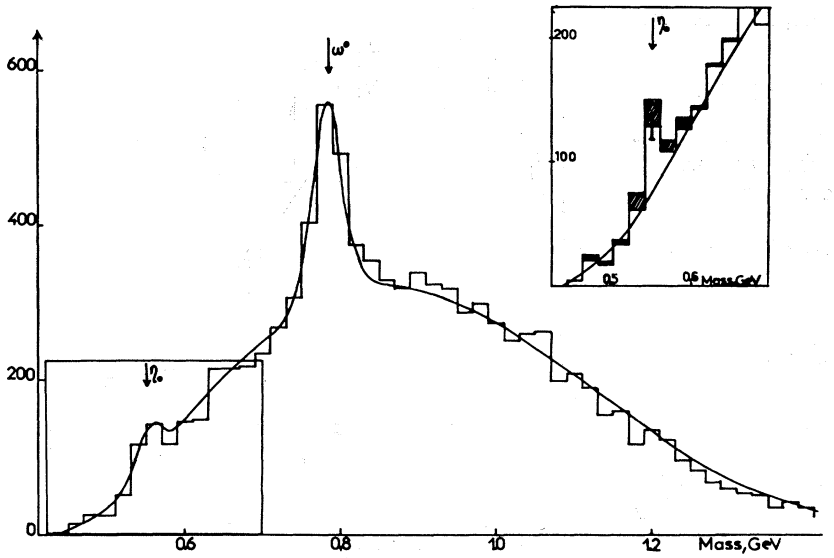

FIG. 10. $\pi^+\pi^-\pi^0$ effective-mass spectrum. The curve shows the best fit obtained with phase-space and Gaussian distributions for the ω^0 and η^0 signals. In inset are shown the details of the η^0 region. Shaded combinations arise from X^0 decays ($0.93<M_{(5\pi)^0}<0.99$ GeV).

The c.m. angular distributions for the $p\pi^+$ and $p\pi^-$ systems in the N^* band (1.12 to 1.30 GeV) have been examined. The distributions do not show significant differences and the backward peaking is very similar to that of the proton distribution [Fig. 3(b)]. In particular, the values of the corresponding asymmetry ratios A_s of -0.37 ± 0.03 for $p\pi^+$ and -0.32 ± 0.03 for $p\pi^-$ are, within the errors, identical with the value -0.34 ± 0.03 for the proton.

For the dipion systems $\pi^+\pi^-$, $\pi^+\pi^+$, and $\pi^-\pi^-$, the c.m. angular distributions for mass combinations in the ρ^0 band (0.67 to 0.85 GeV) were examined. There is forward peaking in each distribution, but there is no significant difference between the $\pi^+\pi^-$ angular distribution, which should reveal the effect of the presence of the ρ^0 meson, and the $\pi^+\pi^+$ and $\pi^-\pi^-$ distributions. The respective asymmetry ratios are 0.19 ± 0.03, 0.17 ± 0.04, and 0.18 ± 0.07.

These features indicate that a considerable proportion of the N^* isobars and the ρ^0 mesons are produced through central collisions. Of course this does not exclude some peripheralism as defined by a Δ^2 dependence, as will be discussed in the next section. However it is clear that the angular distributions offer no possibility of separating a peripheral contribution by comparing the distributions of resonant and nonresonant systems.

3.5 Four-Momentum Transfer Dependence

In low-multiplicity events the peripheral nature of the reactions is most clearly manifested in the four-momentum transfer distributions. In Fig. 9(a) the differential cross section $d\sigma/d\Delta^2$ for the $p\pi^+$ combinations in the N^* band is given, where Δ^2 is the four-momentum transfer squared to the incoming proton. There is evidence for an excess above the predictions of the statistical model in the low four-momentum transfer region for N^* events. No such excess is seen when examining the Δ^2 distribution of the $\pi^+\pi^-$ combinations in the ρ^0 band, where now Δ^2 is the four-momentum transfer squared to the incoming pion.

4. Resonance Production in the Reaction $\pi^+p\rightarrow p3\pi^+2\pi^-\pi^0$

This reaction is dominated by strong N^* and ω production. The X^0 and η mesons are also observed. No other resonances appear.

4.1 N^* Production

In Fig. 7(d) the distribution of the $p\pi^-$ mass combinations is shown. It can be seen that it is fitted very well by phase space without any resonance production. The same is true for the $p\pi^0$ mass distribution. The χ^2 probabilities are 18 and 6%, respectively.

Contrasting with these distributions, the spectrum of $p\pi^+$ mass combinations [Fig. 7(c)] shows a strong deviation from phase space in the N^* region. If the distribution is fitted by use of the modified Breit-Wigner expression,[15] it leads to the result that the N^* isobar is produced in 0.32 ± 0.10 of the interactions. As in the A channel this fit corresponds to a very low χ^2 probability ($\sim10^{-4}$) and this is again partly connected with the shift of the peak by about 20 MeV below its expected value. If the Breit-Wigner expression is modified as in Sec. 2, the resulting χ^2 is then about 20%. Again interpreting the zero-order term of the expansion as being due to N^* leads to an estimate of its production in 0.57 ± 0.08 of the events. The corresponding cross section is 0.35 ± 0.05 mb.

4.2 ω Production and the Dalitz Plot

The distribution of the $\pi^+\pi^-\pi^0$ mass combinations shows an enhancement in the ω region (Fig. 10). It has been checked that the distribution of the other three-

pion charged states (+−−, ++−, etc.) are described reasonably well by pure phase-space calculations. The width of the enhancement in the ω region arises predominantly from the experimental resolution. Fitting in the standard way but representing the ω by a Gaussian distribution, (20 MeV rms), rather than by a Breit-Wigner distribution leads to a value for the proportion of the ω meson of (40±5)%.

As an independent estimate of the proportion of events leading to ω production, the radial density distribution was examined on the Dalitz plot for events in the ω mass region and in the nearby control regions (Fig. 11). For the ω contribution we used the Dalitz plot density[17]

$$\frac{d^2n}{dr^2d\phi} \propto 1-Ar^2-Br^3\cos 3\phi$$

integrated over the ϕ interval kinematically allowed for each r value, the background being represented by a constant as expected from the statistical model (and checked on control regions). Fits were made to determine the proportion of ω mesons in each given mass band. The results are collected in Table IV.

The production of the ω meson is large between the mass limits 753 to 813 MeV. Normalizing to a total number of 1597 events, the proportion of ω mesons is 0.44±0.04. An apparent production of ω mesons is present between 813 and 833 MeV, but whether this is due to a dynamical effect or to measurement and identification errors is not clear. Combining the results of the fit on the $\pi^+\pi^-\pi^0$ mass spectrum and the results on radial density of the Dalitz plot, we estimate the ω rate of production as 0.42±0.04, corresponding to a cross section of 0.26±0.03 mb.

4.3 *The Simultaneous Production of N^* and ω*

From the fraction of $p\pi^+$ mass combinations in an N^* band as a function of the $(\pi^+\pi^-\pi^0)$ effective mass we found a weak constructive correlation between ω and N^* production. The excess above statistical overlap corresponds to (4.6±2.4)% of the events, while complete correlation would give (18±6)%.

TABLE IV. Proportions of ω mesons in different mass bands as deduced from the Dalitz plot of the $\pi^+\pi^-\pi^0$ combinations.

Mass interval (MeV)	Number of combinations	Proportion of ω^0 mesons	χ^2 (9 degrees)	Number of ω^0 mesons
733–753	318	0.00±0.27	11.85	0±86
753–773	429	0.50±0.11	7.47	215±51
773–793	570	0.47±0.07	8.82	268±42
793–813	452	0.51±0.12	7.77	230±51
813–833	374	0.35±0.10	11.20	131±37
833–853	347	0.09±0.11	9.27	31±38
753–813	1451	0.48±0.05	10.90	701±69

[17] G. Källen, *Elementary Particle Physics* (Addison-Wesley, Inc., Reading, Massachusetts, 1964), Chap. 7, p. 202.

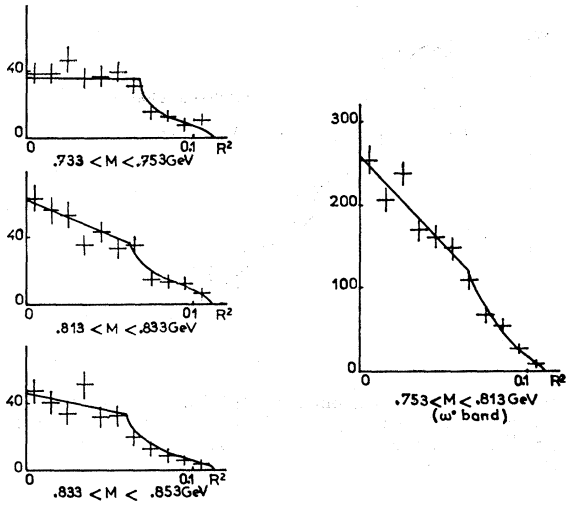

FIG. 11. Radial density of the Dalitz plot for $\pi^+\pi^-\pi^0$ combinations in four mass ranges around the ω^0 mass; $R^2=\frac{4}{3}\{\frac{1}{3}-(T_1T_2+T_1T_3+T_2T_3)/Q^2\}$ with $Q=T_1+T_2+T_3$. The curves correspond to the best fit obtained, assuming ω^0 plus statistical background.

4.4 C.m. *Angular Dependence of Resonance Production*

The angular dependence of resonance production in channel B is very similar to that in channel A. Particle combinations involving a baryon tend to be emitted backwards whereas pion combinations tend to be emitted forwards.

The c.m. angular distributions of $p\pi^+$, $p\pi^-$ combinations in the N^* region are similar, with asymmetry ratios of −0.34±0.02 and −0.28±0.03, respectively. They are seen to be very close to the corresponding value for the proton alone of −0.34±0.02.

In Fig. 12 the asymmetry ratio for the $(\pi^+\pi^-\pi^0)$ combinations is shown for different mass intervals. A significant deviation of this ratio is seen at the ω mass, where the value is 0.32±0.02. For comparison, the average ratio for the charged 3π combinations in the ω band is shown to be 0.23±0.02, in good agreement with the value expected by interpolating the neighboring $\pi^+\pi^-\pi^0$ regions. From the over-all percentage for ω production of 0.42±0.04 the asymmetry ratio for ω mesons only is 0.43±0.05.[18]

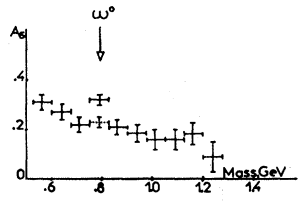

FIG. 12. Asymmetry ratio $(F-B)/(F+B)$ for the $\pi^+\pi^-\pi^0$ combinations as a function of their effective mass. The dotted cross is concerned with the 3π combinations of nonzero charge in the ω^0 mass band.

[18] However, this enhancement in the asymmetry ratio is not pronounced enough to be used as a technique for purifying the sample of ω mesons.

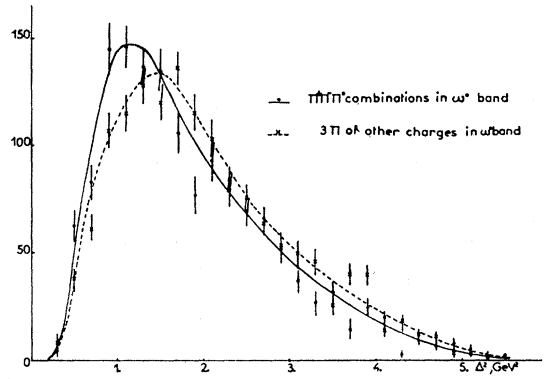

FIG. 13. $\partial N/\partial\Delta^2$ spectrum for $\pi^+\pi^-\pi^0$ combinations lying in the ω^0 band ($0.753<M_{(3\pi)^0}<0.813$ GeV), and for 3π systems of other charges in the same mass interval. The curves are hand drawn.

The tendency for the ω to be emitted more in the forward direction than the background combinations is manifest as a larger forward shift of the central value of the longitudinal momentum for the combinations in the ω band (160 ± 14 MeV/c) than for neighboring mass bands (110 ± 10 MeV/c). However, the narrow concentration of the longitudinal momenta that would be expected for production by glancing collisions is not observed.

4.5 *Four-Momentum Transfer Dependence*

The four-momentum transfer dependence for $p\pi^+$ events in the N^* region is very similar to that in channel A in that again there is evidence for an excess of low Δ^2 values above the predictions of phase space [Fig. 9(b)].

For $\pi^+\pi^-\pi^0$ combinations in the ω mass band, the distribution of Δ^2 is shown in Fig. 13 and is compared with other charge combinations in the same mass band. For the neutral three-pion system it is seen that low Δ^2 values are somewhat more frequent. This tendency of Δ^2 is confirmed by the analysis of the radial density in the $(\pi^+\pi^-\pi^0)$ Dalitz plot.

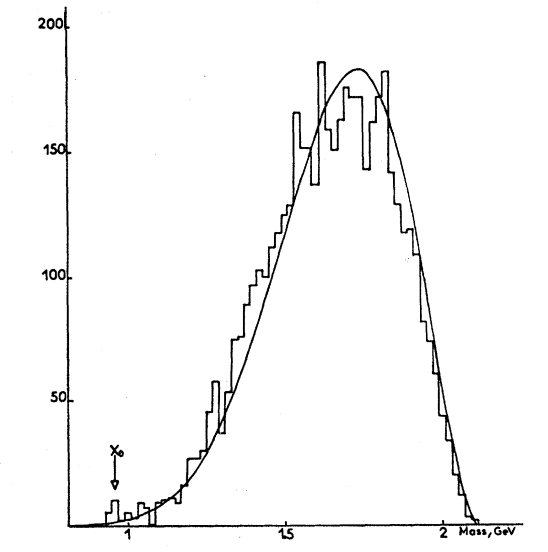

FIG. 14. $\pi^+\pi^+\pi^-\pi^-\pi^0$ effective-mass spectrum. The curve gives phase-space prediction.

4.6 X^0 *Production*

In the effective-mass distribution of the $\pi^+\pi^+\pi^-\pi^-\pi^0$ combinations which is shown in Fig. 14, X^0 production is visible against the low phase-space background. Of the 17 events which contribute to the signal at the X^0 mass (0.93 to 0.99 GeV), 15 are compatible with the decay $X^0\to\pi^+\pi^-\eta$.

From the distribution of these events on the plot of P_L versus P_T (Fig. 15), it is seen that a sizeable fraction of the X^0 events are produced through a peripheral mechanism in association with the N^* isobar.

The cross section for the reaction $\pi^+p\to p\pi^+ X^0$ is 50 ± 20 μb after correction for other decays of the X^0.[19]

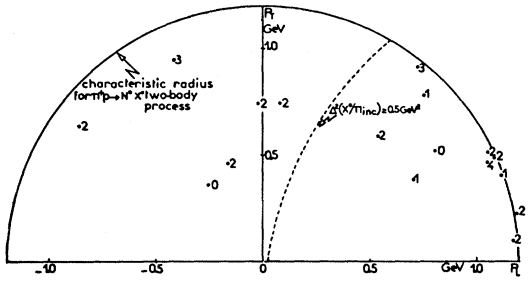

FIG. 15. P_L versus P_T plot for the 17 $\pi^+\pi^+\pi^-\pi^-\pi^0$ combinations lying in the X^0 band ($0.93<M_{(5\pi)^0}<0.99$ GeV). The numbers (from 0 to 4) indicate how many $\pi^+\pi^-\pi^0$ combinations lie in the η^0 mass band ($5.33<M_{(3\pi)^0}<0.563$ GeV).

4.7 η *Production*

In estimating the amount of η production in the $\pi^+\pi^-\pi^0$ mass distribution, events with a 5-pion mass in the X^0 band were first excluded. The effective-mass distribution of the neutral tripion system for the remaining events is shown in the inset of Fig. 10. There is an excess of $\sim$70 combinations in the η region. The total cross section for the reaction $\pi^+p\to p2\pi^+\pi^-\eta$ exclusive of those produced through the X^0 mesons and corrected for neutral decays,[20] is 100 ± 20 μb.

The separation of η mesons from the background in this region is improved if it is demanded that the three contributing pions should each be emitted in a forward cone with a $2\times60°$ opening angle (Fig. 16), implying that a large fraction of η's are produced forward.

[19] G. R. Kalbfleisch *et al.*, Phys. Rev. Letters **13**, 349a (1964); Badier *et al.*, Phys. Letters **17**, 337 (1965); G. W. London *et al.*, Phys. Rev. **143**, 1034 (1966). We used the value 0.12 ± 0.02 for the ratio $X^0\to\pi^+\pi^-\pi^+\pi^-\pi^0$ (or γ)/all X^0.

[20] We took the value 0.27 for the ratio $\eta\to\pi^+\pi^-\pi^0$ (or γ)/all η.

5. Angular Distributions of the Decays of Resonances

In this section the angular distributions involved in the decay of the N^*, ρ^0, and ω in their own rest frames are examined.

5.1 N^* Isobar

As a direct test of whether the N^* isobar is produced through one-pion exchange, the distribution of the angle θ between the ingoing proton and the outgoing proton as seen in the N^* rest system was studied. For one-pion exchange the differential cross section is proportional to $1+3\cos^2\theta$ and should lead to an anisotropy ratio[21] of 0.375. This angular distribution for the N^* band is shown in Fig. 17 where there is no evidence for a $\cos^2\theta$ dependence; moreover the anisotropy ratio is 0.06 ± 0.03 for channel A and 0.08 ± 0.02 for channel B which does not support one-pion exchange.

It was noted that in the N^* region the asymmetry of this angular distribution is smaller for the $p\pi^+$ than

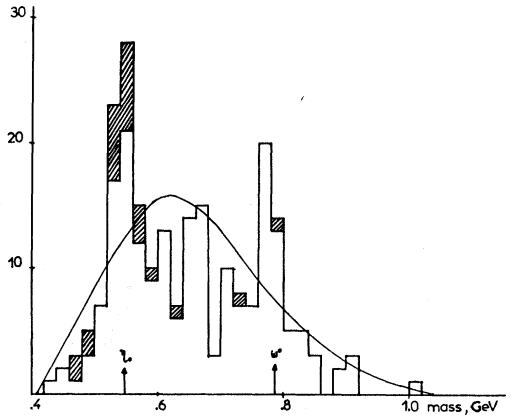

FIG. 16. $\pi^+\pi^-\pi^0$ effective-mass spectrum where each contributing π is requested to be emitted in a forward cone of $2\times60°$ opening angle. Shaded combinations belong to X^0 candidates.

for the $p\pi^-$ combinations. Assuming that the background $p\pi^-$ and $p\pi^+$ combinations have identical asymmetries and that resonant combinations decay symmetrically, an independent estimate of resonance production can thus be made. In this way the proportions of resonance production are 0.81 ± 0.26 and 0.94 ± 0.21 in channels A and B, respectively. Figure 18 indicates that the fraction of the π^+p combinations determined by the symmetric decay criterion extends to higher mass than expected for the $N^*(1236)$.

5.2 ρ^0 Meson

The usual distribution in $\cos\theta$ of the scattering angle of the π^+ was investigated, where θ is defined as the angle between the incident and the outgoing π^+ meson

[21] The anisotropy ratio is defined by $(O-M)/(O+M)$ where M is the number of combinations lying within $-0.5\leq\cos\theta\leq0.5$ and O is the number of events outside this region.

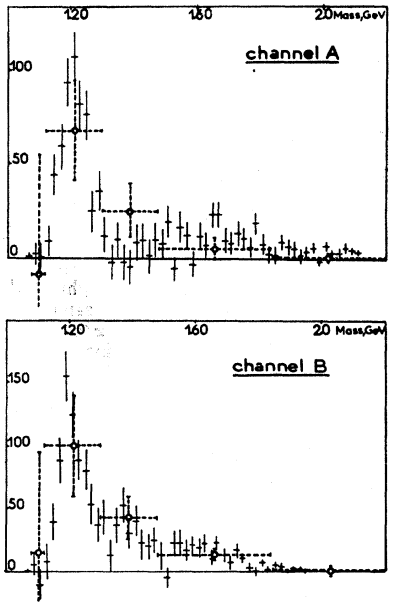

FIG. 18. By comparing the distributions of the decay angle for π^+p and π^-p combinations, the excess of symmetrically decaying π^+p combinations has been estimated for several mass intervals (dotted crosses). The full crosses correspond to the observed excess of π^+p combinations above phase space, as defined in Sec. 6.

in the ρ^0 rest system. No deviation from isotropy was observed.

If one plots the helicity angular distribution $\cos\theta_H$ (where θ_H is the angle between the outgoing π^+ in the ρ^0 frame and the ρ^0 line of flight in the over-all c.m. system), again no significant deviation from isotropy appears. The situation changes, if one selects only those $\pi^+\pi^-$ combinations in the ρ^0 band for which $u>3.0$ GeV^2 [u being defined as the four-momentum transfer squared $(P'-P_{\rm inc})^2$ between the four-momentum P' of the resonant pion combination and $P_{\rm inc}$ of the incoming proton].[22] The result of this selection is given in Fig. 19.

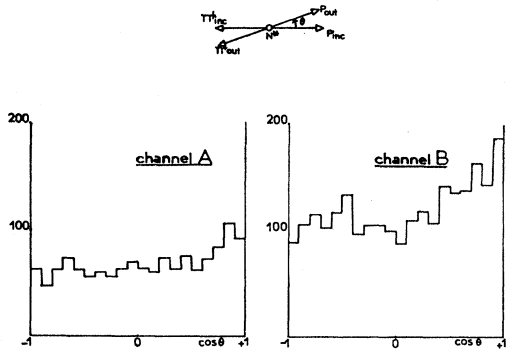

FIG. 17. Decay angle distribution for π^+p combinations lying in the N^* band ($1.12<M_{\pi^+p}<1.30$ GeV) for channels A and B.

[22] It is known that the u parameter might provide a more efficient separation of peripheral contributions than the more usual t parameter.

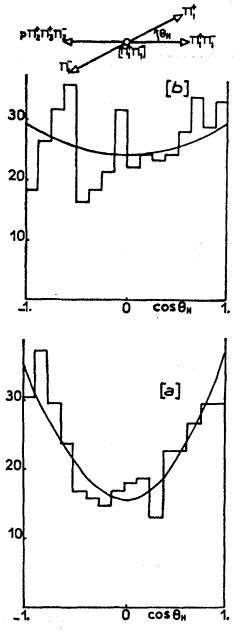

FIG. 19. (a) Decay angle θ_H distribution of the $\pi^+\pi^-$ combinations lying in the ρ^0 band ($0.67<M_{\pi^+\pi^-}<0.85$ GeV). θ_H is the angle, evaluated in the $\pi^+\pi^-$ rest frame, between the outgoing π^+ and the c.m. line of flight of the $\pi^+\pi^-$ system. In (b), the same angle has been investigated for $\pi^+\pi^-$ combinations lying in neighboring mass regions: $0.49<M_{\pi^+\pi^-}<0.67$ GeV and $0.85<M_{\pi^+\pi^-}<1.03$ GeV. All $\pi\pi$ combinations are restricted to $|u|>3.0$ GeV^2. The curves are best fits to $(1-\alpha)+3\alpha\cos^2\theta_H$ (see Sec. II 5.2).

In terms of a fit of the form $(1-\alpha)+3\alpha\cos^2\theta_H$, the value of α is 0.31 ± 0.06 with a χ^2 probability of 81%.

From Fig. 20 it can be seen that the isobar N^* is produced strongly in association with those events in the ρ^0 band which fulfill the above u condition. So in the second step only those $\pi^+\pi^-$ combinations in the ρ^0 band with $u>3.0$ GeV^2 were selected for which at least one of the remaining π^+ mesons forms a $p\pi^+$ combination in the N^* band. Then, $\alpha=0.31\pm0.06$ with a χ^2 probability of 90%. This effect, if real, means that about 20% of the ρ^0 mesons are produced with their spin aligned with respect to the line of flight; the production of the N^* seems to be associated with this alignment.

To investigate whether the effect observed could be from some reflection of the N^* production, we present in Fig. 21(a) the $p\pi^+$ mass distribution for those combinations where the same π^+ is forming a $\pi^+\pi^-$ combination in the ρ^0 band with $u>3.0$ GeV^2. For comparison the $p\pi^-$ mass distribution is given in Fig. 21(b) under the same conditions. No significant differences show up and no appreciable amount of N^* seems to be present in the $p\pi^+$ distribution.

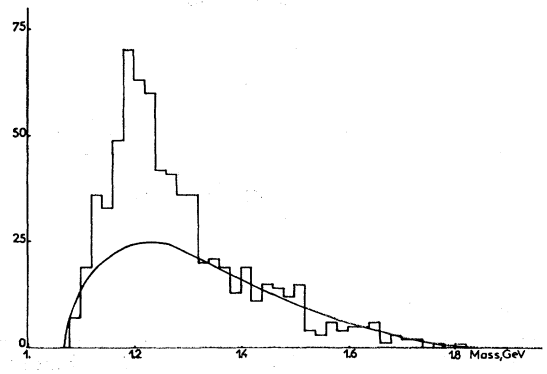

FIG. 20. $p\pi^+$ effective-mass spectrum in channel A restricted to events including a $\pi^+\pi^-$ combination in the ρ^0 band ($0.67<M_{\pi^+\pi^-}<0.85$ GeV) with a u value >3.0 GeV^2. Those $p\pi^+$ are excluded for which the π^+ fulfill these above peripheral ρ^0 conditions.

It has been checked that for the two neighboring $\pi^+\pi^-$ mass bands of width equal to that chosen for the ρ^0 meson, the decay angular distribution in $\cos\theta_H$ is consistent with isotropy. Figure 19(b) shows the result after having added the two distributions.

5.3 ω Meson

Concerning the ω, all relevant angular distributions have been examined. No deviations from isotropy have been observed except for a slight $\cos^2\theta$ dependence of the angle between the incident pion and the perpendicular to the ω decay plane. Fitting with an angular distribution of $(1-\alpha)+3\alpha\cos^2\theta$ yields $\alpha=0.09\pm0.03$ with a χ^2 probability of 4%. (See Fig. 22.) This would correspond to 20% alignment of the ω mesons. The alignment could be evidence for peripheralism; however, the $\cos^2\theta$ effect is not improved when selecting combinations of low-Δ^2 or high-u values.

6. β^* Dependence of Resonance Observations; Short-lived Resonances as a Possible Means to Investigate High-Multiplicity Phenomena

It has been seen in Sec. II.3 and II.4 that the production of resonances, particularly N^*, ρ^0, and ω, contribute largely to channels A and B. In the following, the behavior of these resonances is examined as a function of their c.m. velocity. An attempt is made to demonstrate that, irrespective of any discrepancy of the velocity spectrum of the above resonances with phase-space predictions (a discrepancy possibly connected with a Δ^2 dependence), the observation of these resonances is correlated with their c.m. velocity. In other words, the shape of their effective-mass distributions depends on this velocity (Fig. 24). This effect is first shown with N^* production in channels A and B. Later on, the assumption that there is some connection with the very short lifetime of the N^* is supported by a comparative study of the ρ^0 and ω mesons which have very different lifetimes.

6.1 The Distortion of the π^+p Spectra

The mass spectra of the $p\pi^-$ combinations in channels A and B [Figs. 7(b) and 7(d)] and the $p\pi^0$ combinations in channel B all agree well with the predictions of phase space. In contrasting with this good agreement, the fits to the $p\pi^+$ mass spectra in both channels by the standard method (using Jackson's modifications to the Breit-Wigner formula) are found with very low χ^2 probability (see Sec. II.3.1 and II.4.1). This arises partly from the discrepancy (of about 20 MeV) be-

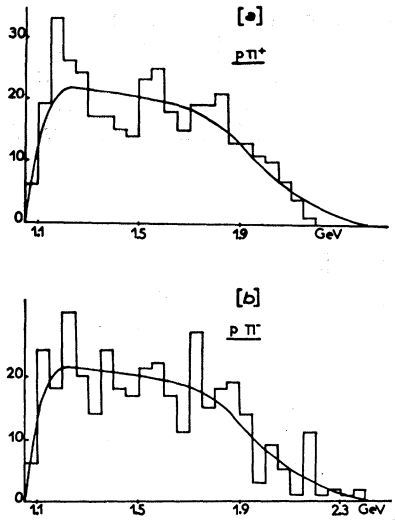

FIG. 21. (a) $p\pi^+$ effective-mass spectrum in channel A; only π^+ which form a $\pi^+\pi^-$ combination in the ρ^0 band ($0.67<M_{\pi^+\pi^-}<0.85$ GeV) with a u value >3.0 GeV^2 are considered. The curve gives the statistical expectation. (b) $p\pi^-$ effective-mass spectrum with similar restrictions.

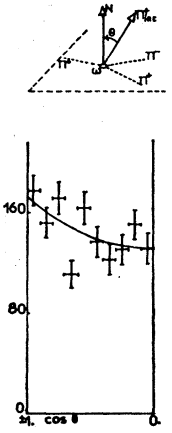

FIG. 22. Folded decay distribution for the $\pi^+\pi^-\pi^0$ combinations lying in the ω^0 band ($0.753<M_{(3\pi)^0}<0.813$ GeV) of the angle between the normal to the decay plane and the incident pion (evaluated in the $\pi^+\pi^-\pi^0$ rest frame). The curve gives the best fit obtained.

tween the observed and expected peaks in the mass spectra and partly from distortions at high masses.

The existence of the higher isobar[23] $N^*(1670)$ could possibly account for the broadening of the mass spectra at higher mass values, as slightly suggested by the π^+p distribution of channel A (Fig. 18). Fits to the $p\pi^+$ mass spectra have been made by including both the $N^*(1236)$ and the $N^*(1670)$; apart from introducing a questionable contribution of 20% from the higher isobar, the fits do not lead to a change in the proportions of the $N^*(1236)$; also the χ^2 probabilities for the fits remain low.

We shall now demonstrate that most of the deviation from expectation is located in the sample of π^+p combinations that have a low c.m. velocity, and that this deviation is certainly not due to experimental biases.

6.2 *The c.m. Velocity of the N^*; the Determination of a Suitable Velocity Cut*

If the statistics allowed it, an examination of the $p\pi^+$ mass spectrum as a function of c.m. velocity would be the best way of examining the problem. Instead it is necessary to divide the combinations into two samples for which the $p\pi^+$ combinations have a high or a low c.m. velocity. The velocity chosen is that which would divide the number of N^* isobars equally between the two velocity samples. However, the method which is

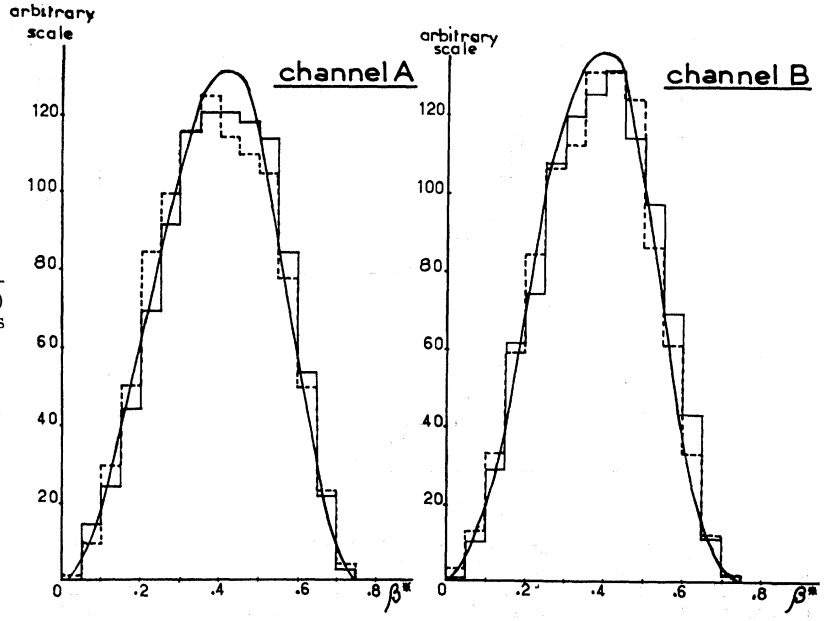

FIG. 23. Center-of-mass velocity distribution for π^+p (full lines) and π^-p (dashed lines) combinations in channels A and B. Curves give statistical predictions.

[23] T. J. Devlin *et al.*, Phys. Rev. Letters **14**, 1031 (1965).

described below will result in the equal division of the "excess over statistical phase space"—hereafter referred to as excess over background–rather than N^* itself.

The c.m. velocity spectrum $P^+(\beta^*)$ of the $p\pi^+$ mass combinations, which can be measured, comprises the velocity $P(\beta^*)$ of the excess above background, which is to be determined, and that of the remaining background $p\pi^+$ combinations. Very likely this latter velocity spectrum is the same as that of the $p\pi^-$ mass combinations $P^-(\beta^*)$. Taking the excess above back-

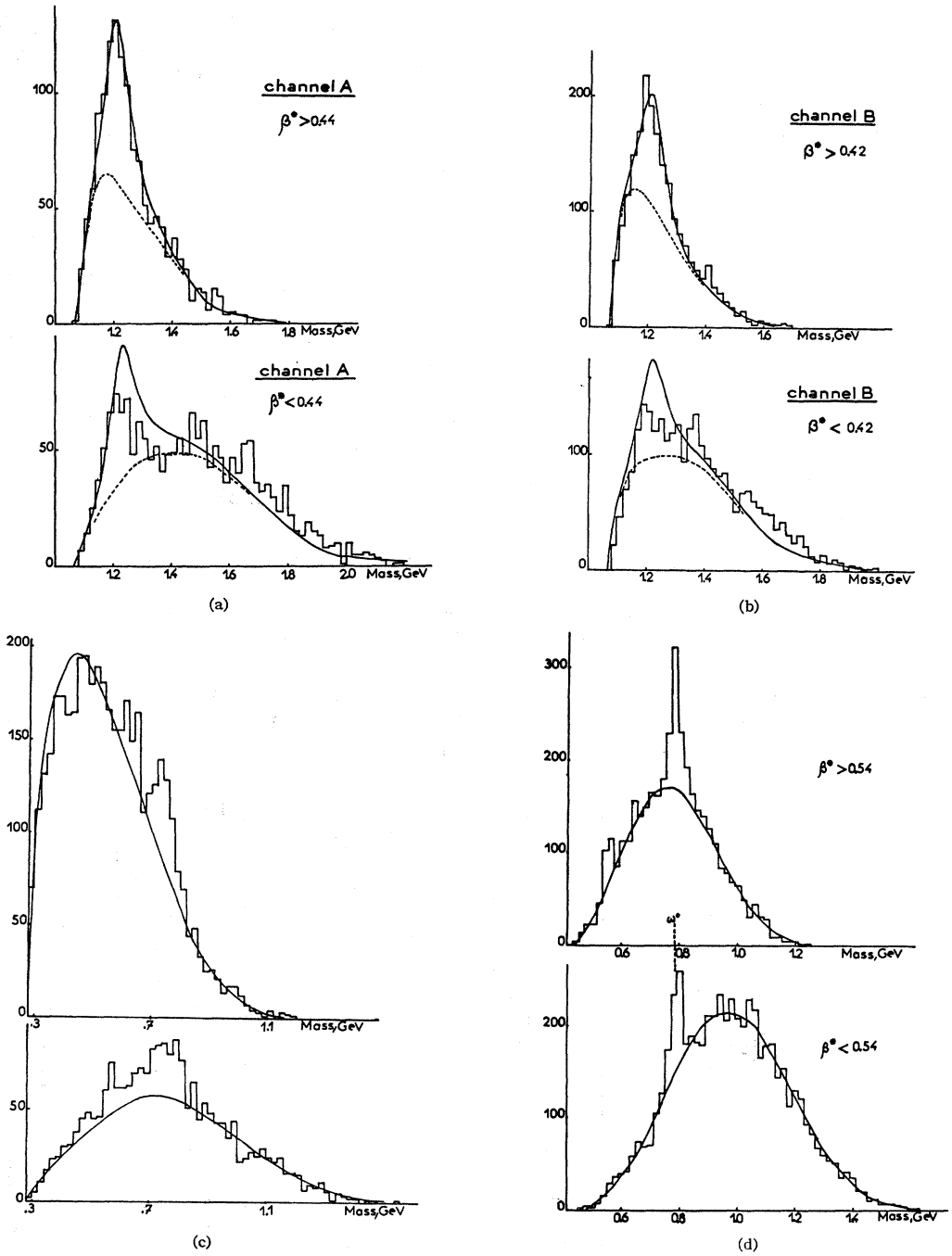

FIG. 24. (a) π^+p effective-mass distributions for two intervals of the c.m. velocity β^*. In the upper diagram, the full line gives the best fit obtained, using phase space and modified Breit-Wigner (Ref. 15); the dashed line gives the level of background as deduced from the same fit. The curves on the low-velocity diagram are deduced from the high-velocity fit, assuming statistical division of the background according to velocity. (b) same for π^+p combinations in channel B. (c) $\pi^+\pi^-$ effective-mass distribution for two ranges of the c.m. velocity β^*. The full curve gives pure phase-space prediction, normalized to nonresonant combinations. (d) $\pi^+\pi^-\pi^0$ effective-mass distribution for two ranges of the c.m. velocity β^*. The full line gives the statistical background, normalized to nonresonant combinations.

ground as δ and considering that there are three $p\pi^+$ combinations in an event, one obtains

$$P(\beta^*)=\delta^{-1}[3P^+(\beta^*)-(3-\delta)P^-(\beta^*)]. \quad (6.1)$$

In Fig. 23 the distributions $P^+(\beta^*)$ and $P^-(\beta^*)$ for each of the channels A and B are shown. The distributions are almost identical and close to the statistical predictions even though $P^+(\beta^*)$ includes the N^* contribution. Hence $P(\beta^*)$ will also be very similar to these and its determination will be insensitive to the value of δ; in the following we set $\delta=0.75\pm0.20$ which value is at this stage rather arbitrary but which will be later justified. Let us mention that $P(\beta^*)$ is quite insensitive to a weak Δ^2 dependence in these high-multiplicity events.[24]

According to the definition of $P(\beta^*)$, the velocity which leads to the equal division of the excess above background is given by

$$\int_0^{\beta} P(\beta^*)d\beta^*=\tfrac{1}{2}.$$

Substituting Eq. (6.1), one obtains the following values of β:

(a) for channel A, $\beta=0.44\pm0.02$;

(b) for channel B, $\beta=0.42\pm0.02$,

where the errors are related to the statistical fluctuations on $P^+(\beta^*)$ and $P^-(\beta^*)$ and to the uncertainties on the values of δ. Using these values of velocity to divide the mass spectra should lead to an equal division (to about 5%) of the excess above background.

The division of the $p\pi^+$ mass combinations into the higher- and lower-velocity subsamples is shown in Fig. 24(a) and 24(b). In each, the phase-space background is drawn. For both channels A and B, it can be seen that the excess above background in the high-velocity sample is about equal to the excess in the low-velocity sample. What is surprising is the large concentration in the N^* region for the higher-velocity samples and the very broad excess for the lower-velocity sample.

If the $p\pi^+$ mass distribution of the higher-velocity sample is now fitted in the standard way using Jackson's modified Breit-Wigner shapes then the proportions a of statistical background in the higher-velocity samples are

(a) channel A: $a=(0.70\pm0.03)$ with a $P(\chi^2)\sim50\%$;

(b) channel B: $a=(0.73\pm0.03)$ with a $P(\chi^2)\sim20\%$.

The χ^2 probabilities are now much larger than in the corresponding fits to the mass spectrum of all events. In particular, this is because the predicted peak of the mass spectrum corresponds more closely to the observed one (since phase space peaks now at a lower value). Hence, by selecting events in the higher-velocity interval, the excess above background concentrates almost exactly in the region where the N^* is expected to appear. For the lower-velocity samples, the fitting remains poor. Even if the fitting is restricted to the N^* region, the χ^2 probabilities are still very low.

Suppose that the N^* isobars have been divided equally by the velocity sampling. If so, most of the excess above background in the lower-velocity sample would arise from the production of N^* isobars that have undergone some further physical process which distorts the mass spectrum. Then, from the above a and assuming statistical repartition of the $p\pi^+$ background, the proportions of initial N^* isobars in the whole sample are 0.78 ± 0.11 and 0.70 ± 0.08 for channels A and B, respectively. These values are similar to those obtained by the excess above background fitting with the expanded Breit-Wigner shape described in Sec. II.3.1 and with the results of angular decay analysis in Sec. II.5.1.

There exists a correlation, although a rather weak one, between the low c.m. velocities and high velocities in the laboratory system. This suggests that the effect here discussed might be due to misclassification of the proton, which is likely to affect events with fast protons. We checked that the sample of events with proton momentum larger than 1.5 GeV/c do show a clear N^* signal, implying that the strong distortion in the low-velocity subsample cannot be explained in this way.

By examining the production of N^* isobars with velocity, it has been possible to associate the distortion of the mass spectra with low velocities. Indeed the χ^2 probability of fitting has increased considerably in the higher-velocity sample where the discrepancy between the calculated and observed position of the mass peaks has been almost completely removed.

Of course the problem of the distortion of the over-all mass spectrum remains, but it is now seen to be a characteristic of low velocities. A tentative interpretation based on similar analysis of the neutral dipion and tripion systems is discussed below.

6.3 The ρ^0 and ω Mesons

A detailed study of the shape of the ρ^0-meson peak as a function of its c.m. velocity is difficult because of the position of the ρ^0 peak in the $\pi^+\pi^-$ mass spectrum, the high number of $\pi^+\pi^-$ combinations (6) which enter the plots for each event, and an appreciable distortion arising from the reflection of the ρ^0 on the plot, which is itself related to $p\pi^+\rho^0\pi^+\pi^-$ and $N^*\rho^0\pi^+\pi^-$ events.

For the samples of $(\pi^+\pi^-)$ and $(\pi^+\pi^-\pi^0)$ mass combinations, a velocity of $\beta=0.54$ was chosen which according to the statistical model would divide the ρ^0

[24] A certain Δ^2 dependence causing a forward depopulation as well as a backward over population of protons does not modify significantly the velocity spectrum [see Fig. 3(a)].

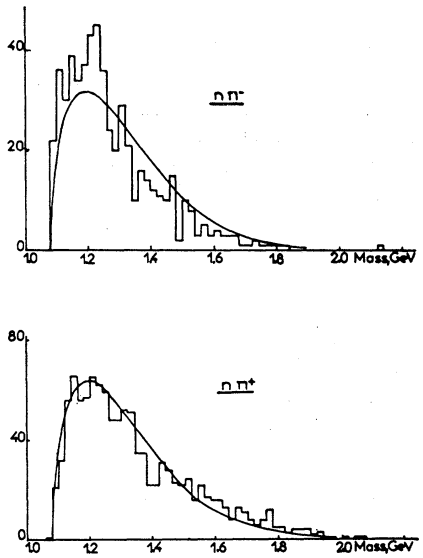

FIG. 25. $n\pi^+$ and $n\pi^-$ effective-mass distributions in channel *C*. The curves give phase-space predictions normalized to all events.

and ω mesons about equally (neglecting the velocity dependence of production of these resonances).

In the higher-velocity samples shown in Figs. 24(c) and 24(d) the ρ^0 and ω peaks, respectively, are clearly seen. The $\pi^+\pi^-$ and $\pi^+\pi^-\pi^0$ pure phase-space background (full curves) is normalized on the basis of 63% ρ^0 and 42% ω production. The ω signal is as clearly resolved in the lowest-velocity sample as in the high-velocity sample, while this is not true for the ρ^0.[25]

6.4 Possible Implications

The dependence on velocity of the three resonances which are produced most abundantly in six-prong events has been examined. For the N^* and possibly for the ρ^0, it has been seen that the distortions of the $p\pi^+$ and $\pi^+\pi^-$ mass spectra are associated with low velocities.[26] For the ω no such effect is observed.

For the N^* and ρ^0, at an average velocity of $\sim$0.5, the mean decay length is $\sim$1 F which is typical of the range of nuclear forces; the decay length of the ω is some 10 times larger. Perhaps it is not surprising that the velocity of these resonances is a relevant parameter in the dynamical description of the six- or seven-bodied systems. Velocity is a frame-dependent quantity and the effect, being sensitive in the c.m. system, implies that this is the proper frame for the description of these events, or at least is not far from it.

The specific characteristics, that is, weakening of the signals and alteration of their shape, suggest an "erosion" effect. Such an "erosion" would occur if resonances were produced directly (i.e., not by final-state interaction), the reinteraction of their decay products with the surrounding pionic field distorting (eroding) the mass shape. This scheme is far from being established but merely suggested by the present observations. That the ρ^0 and ω are produced directly and not by secondary interactions is borne out by the striking equality of ρ^0 and ω production in quasi-identical kinematical configurations, i.e., the ratio of ρ^0 to ω production remains of order 1, from 5 GeV/c (this experiment) through 6.9 GeV/c [3] to 8 GeV/c.[5,27]

7. The Neutron and NO-FIT Channels

7.1 Resonance Production in the Channel $\pi^+p \to n4\pi^+2\pi^-$

The population (279 events) of the channel $n4\pi^+2\pi^-$ is relatively weak compared to the channels $p3\pi^+2\pi^-$ and $p3\pi^+2\pi^-\pi^0$ (cf. Table I). The only resonance which makes a significant contribution to the effective-mass plots is the $N^{*-}(1236)$ in the $n\pi^-$ distribution. In Fig. 25, the $n\pi^+$ and the $n\pi^-$ effective-mass distributions are given for comparison.

The result of a fit obtained in a way analogous to that described for reaction *A* is that a fraction of (60±25)% of the events form an isobar $N^{*-}(1236)$. The corresponding cross section is 0.07±0.03 mb.

The production angular distribution for the $n\pi^-$ combinations in the N^* band does not show any significant difference from the corresponding distribution for the $n\pi^+$ combinations. The backward peaking of the neutron (A_s=0.42±0.07, see Table II) reflects itself in a backward peaking of the combinations in the N^* band with asymmetry ratios −0.50±0.05 for the $n\pi^-$ combinations and −0.50±0.04 for the $n\pi^+$ combinations. Also no significant difference can be observed

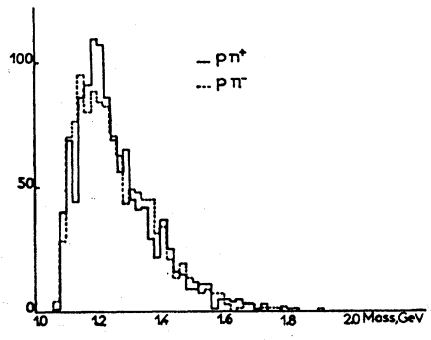

FIG. 26. $p\pi^+$ and $p\pi^-$ effective-mass distributions in channel *D*.

[25] It may be noticed that the ρ^0 signal for high-velocity sample is somewhat narrower than the currently reported width (120 MeV).

[26] This effect might have some relation with the transfer dependence of the ρ^0 width suggested by Ross *et al.* and investigated by James *et al.* in $\pi^+p \to p\rho^+$ at 2.0 GeV/c; M. Ross and G. Shaw, Phys. Rev. Letters **12**, 627 (1964); F. E. James and H. L. Kraybill, Phys. Rev. **142**, 896 (1966).

[27] This equality seems no longer true at 4 GeV/c (Ref. 4) (0.20± 0.04 mb for ω and less than 0.10 mb for ρ^0) but this may be a threshold effect.

between the four-momentum transfer distributions for the $n\pi^-$ and $n\pi^+$ combinations in the N^* band.

7.2 The Channels D and E

Only a relatively small number of events (cf. Table I) contributes to the channels $p3\pi^+2\pi^-(m\pi^0)$ and $n4\pi^+2\pi^-(l\pi^0)$ with $m\geq 2$ and $l\geq 1$. No significant resonance production has been detected in these two channels, with the exception that there are indications for some $N^*(1236)$ production in the D channel. The effective-mass distributions for the $p\pi^+$ and the $p\pi^-$ combinations in this channel are given in Fig. 26. No phase-space calculation, which is possible only with further assumptions about the multiplicity of additional neutral pions, has been done. From the difference of the shape of the $p\pi^+$ and the $p\pi^-$ mass spectra, one obtains an estimate of about $(30\pm 20)\%$ of the events forming an $N^*(1236)$.

III. CONCLUSIONS

In studying 3502 six-charged-prong π^+p interactions at 5 GeV/c, it was first noted that the most populated channels are characterized by the fact that the proton retains its charge and that rarely is more than one π^0 present. This paper has then been mostly concerned with the corresponding A and B channels: $\pi^+p\rightarrow p3\pi^+2\pi^-$ and $\pi^+p\rightarrow p3\pi^+2\pi^-\pi^0$.

A very general feature of these reactions is already revealed by the study of individual final-state particles. It is found that no glancing collisions contribute to these phenomena (with the exception of the weak N^*X^0 peripheral production). However, the momentum distributions do not quite follow the relativistic statistical phase space; the average momentum of the nucleon is nonzero in the c.m. system and points backward, correlatively the average pion momentum is nonzero and points slightly forward. Moreover the average transverse momentum is in all cases slightly smaller than expected. This could be the onset of a limitation on transverse momenta often reported at higher energies.

Despite the over-all statistical character of the observations on individual particles, the study of mass plots reveals abundant production of N^{*++} and ρ^0 in channel A as well as N^{*++} and ω in channel B with a weak transfer dependence, if any. In neither of these two cases has it been possible to establish that these productions are significantly correlated. N^* cross sections seem to be of the same order of magnitude in both channels and ρ^0 and ω cross sections are also quite similar. Besides these three resonances one observes η and X^0 (mostly forward) in channel B and possibly $f^0\rightarrow 4\pi$ in channel A. It must be noted that no other resonance states show up in the mass plots, in particular N^* and ρ are only observed in the above-mentioned charge states. We give in Table V the cross sections for the observed resonance production as well as upper limits (95% confidence level) for some resonant states which are not observed.

TABLE V. Resonance cross sections for channels A and B. Upper limits are given within a 95% level.

Resonance		Observed decay	Cross section channel A (mb)	Cross section channel B (mb)
$N^*(1236)$	$++$	$\rightarrow p\pi^+$	0.25 ± 0.05	0.35 ± 0.05
	$+$	$\rightarrow p\pi^0$	...	<0.02
	0	$\rightarrow p\pi^-$	<0.02	<0.03
$\eta(549)$[a]		$\rightarrow \pi^+\pi^-\pi^0$ corrected for neutral decay	...	0.027 ± 0.006 0.10 ± 0.02
$\omega(783)$		$\rightarrow \pi^+\pi^-\pi^0$	...	0.26 ± 0.03
$X^0(958)$		$\rightarrow \pi^+\pi^+\pi^-\pi^-\pi^0$ corrected for others decays	...	0.006 ± 0.002 0.05 ± 0.02
$\rho(760)$	$+$	$\rightarrow \pi^+\pi^0$	...	<0.02
	0	$\rightarrow \pi^+\pi^-$	0.26 ± 0.05	<0.03
	$-$	$\rightarrow \pi^-\pi^0$	...	<0.015
$A1(1080)$	$+$	$\rightarrow \pi^+\pi^+\pi^-$	<0.03	<0.03
	0	$\rightarrow \pi^+\pi^-\pi^0$	...	<0.03
	$-$	$\rightarrow \pi^-\pi^+\pi^-$	<0.02	<0.02
	$+$ or $-$	$\rightarrow \rho^0\pi^+$ & $\rho^0\pi^-$	<0.03	...
$A2(1300)$	$+$	$\rightarrow \pi^+\pi^+\pi^-$	<0.02	<0.015
	0	$\rightarrow \pi^+\pi^-\pi^0$	...	<0.01
	$-$	$\rightarrow \pi^-\pi^+\pi^-$	<0.01	<0.01
	$+$ or $-$	$\rightarrow \rho^0\pi^+$ & $\rho^0\pi^-$	<0.02	...
$B(1210)$	$+$	$\pi^+\pi^+\pi^-\pi^0$	...	<0.04
	$-$	$\pi^-\pi^+\pi^-\pi^0$	...	<0.03
	$+$ or $-$	$\omega\pi^+$ & $\omega\pi^-$	...	<0.025
$f^0(1250)$		$\rightarrow \pi^+\pi^-$	<0.005	<0.001

[a] Exclusive of those produced through the X^0 mesons.

There are indications for spin alignments concerning the ρ^0 and ω relative to the line of flight of the resonance in the first case and to the incident pion direction in the second.

In the total sample it appears that the N^* signal in both channels A and B is not correctly described by the Breit-Wigner function as modified by Jackson.[15] It is shown that these deviations can be located in the samples of low c.m. N^* velocity. Since slow N^* have a mean free path before decay which is less than 1 F (which dimension is typically ascribed to the interaction range), it is suggested that this effect has a direct relation to the short lifetime of the N^*. Indeed, such a dependence seems to affect the short-lived ρ^0 and not the comparatively long-lived ω.

The present work remains all along essentially descriptive and we rarely have at hand any framework into which these observations would fit. The understanding of high-multiplicity phenomena is not very advanced at the present time and it is not clear to us which one of the reported results is likely to contribute the most to further development.

ACKNOWLEDGMENTS

We are very much indebted to the staff of the CERN proton synchrotron and to the crew of the

BNHBC. We thank the Institut für Instrumentelle Mathematik at Bonn, and the FIAT Company at Torino for computer time.

We would like also to acknowledge Dr. Vanderhaghen for his efficient contribution when the experiment started.

The Durham group wishes to thank the Science Research Council for over-all support while the Bonn group acknowledges financial support from the Bundesministerium für Wissenschaftlich Forschung. This work has profited from several stimulating discussions with members of the CERN theoretical and TC divisions. It is a pleasure to record the efforts of our scanning and measuring teams.

PHYSICAL REVIEW VOLUME 161, NUMBER 5 25 SEPTEMBER 1967

Polarization Parameter in Elastic Proton-Proton Scattering from 0.75 to 2.84 GeV*

HOMER A. NEAL† AND MICHAEL J. LONGO
The University of Michigan, Ann Arbor, Michigan
(Received 31 March 1967)

The polarization parameter in elastic proton-proton scattering has been measured at 0.75, 1.03, 1.32, 1.63, 2.24, and 2.84 GeV by employing a double-scattering technique. An external proton beam from the Brookhaven Cosmotron was focused on a 3 in.-long liquid-hydrogen target and the elastic recoil and scattered protons were detected in coincidence by scintillation counters. The polarization of the recoil beam was determined from the azimuthal asymmetry exhibited in its scattering from a carbon target. This asymmetry was measured by a pair of scintillation-counter telescopes which symmetrically viewed the carbon target. The analyzing power of this system was previously determined in an independent calibration experiment employing a 40%-polarized proton beam at the Carnegie Institute of Technology synchrocyclotron. False asymmetries were cancelled to a high order by periodically rotating the analyzer 180° about the recoil beam line. Spark chambers were utilized to obtain the spatial distribution of the beam as it entered the analyzer; this information allowed an accurate determination of the corrections necessary to compensate for any misalignment of the axis of the analyzer relative to the incident-beam centroid. Values of the polarization parameter as a function of the center-of-mass scattering angle are given for each incident beam energy. The predictions of the Regge theory for polarization in elastic proton-proton scattering and recently published phase-shift solutions are compared with the experimental results. Surprisingly good agreement with the Regge predictions is found despite the low energies involved.

I. INTRODUCTION

THE polarization parameter in elastic proton-proton scattering at 0.75, 1.03, 1.32, 1.63, 2.24, and 2.84 GeV was measured in a double-scattering experiment performed at the Brookhaven Cosmotron. While the differential scattering cross section for elastic p-p collisions is well known in the region 1 to 3 GeV, there was until recently a marked scarcity of corresponding polarization measurements. In this region, polarization data have been reported by Grannis *et al.*[1] at 1.7 and 2.85 GeV, by Bareyre *et al.*[2] at 1.7 GeV, and by Ducros *et al.*[3] at 1.03 and 1.19 GeV; however, the results of the two experiments at 1.7 GeV appear to be inconsistent. Preliminary results of the present experiment were reported in an earlier paper by the present authors.[4]

In general, the central goal in the study of the proton-proton system is the construction of the complete scattering matrix for proton-proton collisions. The measurement of the necessary number of independent spin-correlation parameters to unambiguously determine the scattering matrix is currently experimentally prohibitive. However, cross-section and polarization data alone can impose stringent conditions on any theoretically predicted phase shifts. On the other hand, cross-section and polarization data can be used in conjunction with physical models to predict the possible phase-shift solutions. The latter approach has been employed by Hama, who used one-boson and one-pion exchange models to obtain phase-shift solutions for the

* Work supported by the U. S. Office of Naval Research under Contract No. Nonr-1224(23).

† National Science Foundation Postdoctoral Fellow at CERN, Geneva. Permanent address: Department of Physics, Indiana University, Bloomington, Indiana.

[1] P. Grannis, J. Arens, F. Betz, O. Chamberlain, B. Dieterle, C. Schultz, G. Shapiro, H. Steiner, L. van Rossum, and D. Weldon, Phys. Rev. **148**, 1297 (1966).

[2] P. Bareyre, J. F. Detoeuf, L. W. Smith, R. D. Tripp, and L. van Rossum, Nuovo Cimento **20**, 1049 (1961).

[3] Y. Ducros, A. de Lesquen, J. Movchet, J. C. Raoul, L. van Rossum, J. Deregel, J. M. Fontaine, A. Boucherie, and J. F. Mougel, submitted to the Oxford International Conference on Elementary Particles, 1965 (Rutherford High Energy Laboratory, Harwell, England, 1966). G. Cozzika, Y. Ducros, A. de Lesquen, J. Movchet, J. C. Raoul, L. van Rossum, J. Deregel, and J. M. Fontaine, submitted to the Thirteenth International Conference on High-Energy Physics, Berkeley, California, 1966 (University of California Press, Berkeley, California, 1967).

[4] Michael J. Longo, Homer A. Neal, and Oliver E. Overseth, Phys. Rev. Letters **16**, 536 (1966).